

NASA Technical Memorandum 106947  
AIAA-95-1880

# Further Investigations of Icing Effects on an Advanced High-Lift Multi-Element Airfoil

Dean Miller, Jaiwon Shin, and David Sheldon  
*National Aeronautics and Space Administration*  
*Lewis Research Center*  
*Cleveland, Ohio*

Abdollah Khodadoust and Peter Wilcox  
*McDonnell Douglas Aerospace*  
*Long Beach, California*

Tammy Langhals  
*NYMA, Inc.*  
*Engineering Services Division*  
*Brook Park, Ohio*

Prepared for the  
Applied Aerodynamics Conference  
sponsored by the American Institute of Aeronautics and Astronautics  
San Diego, California, June 19-22, 1995



National Aeronautics and  
Space Administration

# FURTHER INVESTIGATIONS OF ICING EFFECTS ON AN ADVANCED HIGH-LIFT MULTI-ELEMENT AIRFOIL

Dean Miller  
Jaiwon Shin  
David Sheldon  
NASA Lewis Research Center

Abdollah Khodadoust  
Peter Wilcox  
McDonnell Douglas Aerospace

Tammy Langhals  
NYMA, Inc.

## ABSTRACT

In 1993 an experimental effort was initiated to investigate the effect of ice accretions on an advanced high-lift, multi-element airfoil. This airfoil is representative of an advanced transport wing, and has a state-of-the art three element high lift system. This experimental effort is part of a cooperative program between McDonnell Douglas Aerospace and the NASA Lewis Research Center. The goal of this program is to improve the current understanding of ice accretion characteristics on multi-element airfoils.

One key objective of this program is to establish an experimental database of multi-element ice accretions using the NASA-Lewis Icing Research Tunnel (IRT). The first multi-element icing test in this cooperative effort was conducted in 1993. A second "follow on" icing test was conducted in 1994, for the purpose of augmenting the multi-element ice accretion database obtained in 1993, and also for studying the effect of flap gap setting on ice accretions. This paper presents selected results from the 1994 multi-element icing test, and will emphasize the effect of angle-of-attack, and flap gap setting on multi-element ice accretions.

## NOMENCLATURE

c	Stowed airfoil chord length, inch
t	Ice accretion time, minutes
$T_s$	Static air temperature, °F
$T_t$	Total air temperature, °F
V	Airspeed, mph
x	Chordwise axis
y	Axis normal to the x-axis
$\alpha$	Angle-of-attack, degrees
LWC	Liquid water content, $g/m^3$
MVD	Median volume droplet diameter, $\mu m$

## INTRODUCTION

With changes in financial requirements in the airline industry, aircraft manufacturers have been working to improve the performance, while simplifying the design of high lift systems. This has led to aft-loaded wing designs with fewer high lift devices; often a slat, and a large-chord single-segment flap. Development of such an airfoil has been carried out by McDonnell Douglas Aerospace (MDA) in the Low Turbulence Pressure Tunnel (LTPT) at the NASA Langley Research Center.<sup>1-4</sup> The maximum lift capability of these designs are quite sensitive to the flap-to-spoiler rigging, so there was concern that any ice accretion might have a significant impact.

To address this environmental contamination issue, a cooperative program between McDonnell Douglas Aerospace and the NASA Lewis Research Center was initiated in 1993. The objective of this effort was to improve the understanding of ice accretion effects on multi-element airfoils. Multi-year icing tests were planned as part of a comprehensive development effort for advanced high-lift, multi-element airfoils by MDA.<sup>5</sup>

The first icing test on the advanced MDA multi-element airfoil design was conducted in the IRT during the summer of 1993. The objectives of this test were: (1) to acquire ice accretion data on a high-lift, multi-element airfoil for various configurations including the landing configuration for CFD validation and planned future aerodynamic performance tests, (2) to investigate susceptibility of ice build-up on flaps of an advanced multi-element airfoil with optimized flap gaps, and (3) to investigate effects of an anti-iced slat on ice accretions on the downstream elements.

Some of the more noteworthy findings from this test are listed below:<sup>5</sup>

1. Slat ice accretions were sensitive to the change in icing parameters much like the leading edge of a single element airfoil. However, ice accretions on the main element and the flap were much less sensitive to the change in icing parameters.
2. Slat anti-icing had very little effect on ice accretions on the downstream elements for the icing conditions tested.
3. For all icing conditions tested, the entire lower surface of the flap accreted ice. Ice accretion at the trailing edge of the flap was significant for most cases.
4. Gaps between the elements were never contaminated for the icing conditions and flap settings that were tested. Ice generally accreted away from the gap preventing the gap from being filled by the ice accretion.

The second icing test of the MDA / NASA cooperative program was conducted during the summer of 1994. Its objectives were essentially the same as those for the 1993 test, with the addition of investigating the effect of the flap gap size on multi-element ice accretions.

This paper presents results from the 1994 IRT test of the multi-element model. The scope of this paper will be limited to investigating the effect of the angle-of-attack, and also the effect of flap gap setting on the multi-element ice accretions. Clean multi-element airfoil pressure distributions obtained in the IRT, will also be presented.

## DESCRIPTION OF TEST

### Icing Research Tunnel

The NASA IRT is a closed-loop refrigerated wind tunnel. A 5000 hp fan provides airspeeds up to 400 mph (empty test section). The refrigeration heat exchanger can control the air temperature from ambient temperature to -20°F. The spray nozzles provide droplet sizes from approximately 15 to 40  $\mu\text{m}$  median volume droplet diameters (MVD) with liquid water contents (LWC) ranging from 0.3 to 3.0  $\text{g}/\text{m}^3$ . The test section of the tunnel is 6 ft high and 9 ft wide. Figure 1 shows the schematic view of the IRT.

### Model

The model is a two-dimensional multi-element airfoil model designed and fabricated specifically for vertical installation in the IRT. The current model can be assembled in a number of different three-element configurations. The cruise wing configuration has a nominal span of 71.75 inches and a chord of 36 inches. For this test entry, however, no accommodations were provided for assembling the model in the cruise configuration. Model parts available for testing include a slat with a hot-air anti-ice system, a main element assembly, and flap components which can be assembled into four different configurations. A total of 128 static pressure orifices are available for hookup at one time for the three-element model. Pressure orifice rows include a single row at midspan and spanwise rows on the upper surface of the slat and flap elements only.

The high-lift components of the model are rigged to the main element each with a set of four one-piece steel brackets. These brackets set a baseline combination of deflection, overhang, and gap. Figure 2 shows how deflection, overhang and gap are physically defined on the multi-element model.

Deflection is defined as the angle between the main element wing reference plane (WRP) and the deflected component WRP. Overhang is defined as the horizontal distance (i.e., parallel to the main element WRP) between the trailing edge of one element and the leading edge of the downstream element.

Gap is defined as the minimum distance, in any direction, between the trailing edge of an element and the downstream element. Gap variation through vertical translation only is obtained by installing or removing a set of four constant thickness shims between the brackets and the main element. Two sets of slat brackets, three sets of flap brackets, and a variety of shim thicknesses are available for this entry.

Slat: The leading edge slat is a conventional type slat fabricated of aluminum. Installed internally in the hollow slat is a hot air anti-ice system consisting of a 0.5 inch outside diameter porous steel pipe manifold sealed at its downstream end. A source external to the test section provides hot air into the manifold up to a maximum of 300°F to maintain approximate slat surface temperatures of 100°F in the slat leading edge region and above 32°F over the remaining external surface of the slat. Sets of brackets are available to support and rig the slat to the main element at deflections of 20 and 30 degrees and a set of 0.090 inch

shims is provided to vary the vertical height of the slat with respect to the main element. The slat has 35 chordwise and 6 spanwise static pressure orifices, and 4 thermocouples installed in the leading edge.

**Wing Main Element:** The aluminum main element is comprised of a main spar with removable Wing-Under-Slat-Surface (WUSS), main spar, spoiler, and Bent-Up-Trailing-Edge (BUTE) components. The wing spar is designed to accommodate the installation of support brackets for the high-lift components. Allowances have also been made for the exit of pressure tubing (flap and slat) and thermocouple leads (slat only) from the lower surface side of the model through the lower tunnel turntable with minimal interference to the local freestream. The main element has 42 chordwise and no spanwise static pressure orifices.

**Flap:** An aluminum flap assembly was tested during the entry. The configuration is a two-piece assembly comprised of a forward component and an aft component. The forward section represents the VF90B (non-proprietary conventional leading edge), while the aft section represents a stowed auxiliary flap with a conventional trailing edge (AUX). The flap assembly has 33 chordwise pressure orifices and a total of 12 spanwise pressure orifices in two rows; one in the forward and the other in the aft component.

#### IRT Pressure Measurement System

The model surface pressures were measured with the IRT facility Electronic Scanning Pressure system (ESP). The ESP system offers a transducer per measurement to produce high data rates for multiple pressure measurements with errors no greater than  $\pm 0.10$  percent of full scale. This is accomplished by a three point pressure calibration to all port transducers. Each calibration pressure is measured with a precision digital quartz transducer. The standard calibration interval is every 400 cycles (approximately 15 minutes). The reference pressure to the ESP system is located outside of the tunnel balance chamber due to static pressure changes within the chamber. The balance chamber which is vented to the test section sees the local static pressure.

The ESP system capacity was expanded to include six 32-port ( $\pm 5$  psid) modules for a total of 192 pressure channels for this test. A check pressure applied to port 1 of each module was used to initiate ESP transducer calibration when its level deviated beyond a threshold of  $\pm 0.05$  psi.

#### Test Method:

The icing test was conducted to obtain ice shape data for two main purposes: for scaled icing conditions (SCALING runs), and for numerical code validation (CFD runs).

The SCALING runs were intended to obtain multi-element ice accretions under simulated continuous maximum icing conditions. The full-scale icing conditions were selected from the section of the Federal Aviation Regulations (FAR) containing the envelopes of icing conditions (FAR part 25). The method of Ruff was then used to obtain the scaled icing conditions for the SCALING runs.<sup>5,6</sup>

CFD runs were made to generate a database for code validation at takeoff and landing configurations for a variety of icing conditions. All pressure distribution and ice shape data presented herein were obtained during "CFD runs" with the multi-element model in the landing configuration.

Prior to testing each configuration for icing, surface pressure measurements were made with the clean airfoil at various angles-of-attack. During the pressure measurement, the airfoil was rotated from  $-4$  to  $16$  degrees angle-of-attack in  $4$  degree increments. The airfoil was not tested at angles higher than  $16$  degrees angle-of-attack because target airspeeds could not be obtained due to the tunnel blockage generated by the airfoil.

To measure the contour of the accreted ice on each element, a simple tracing technique was used. After completion of each icing run, slices were made in the ice with heated aluminum plates at each measurement location. Once all the ice had been removed at each location, a cardboard template cut to the shape of the airfoil surface was inserted into the cut. Using a sharp pencil and insuring that the side of the lead was kept in contact with the ice, the accreted ice shape was traced onto the cardboard template. Ice shape tracings were taken at two spanwise locations for all runs.

To improve the accuracy of this technique, two precision items were used. First, the slices in the ice were made with aluminum plates which had been wire cut to the exact coordinates of the airfoil. This helped to assure that the ice was completely melted in each slice. Second, the tracing templates were cut by precision rule die. The resulting tracing templates were uniform and true to the airfoil surface. In addition, two reference points were cut into the tracing templates by the die. These reference points allowed

exact positioning of the measured ice shape in relation to the airfoil after the tracing had been digitized and stored onto a computer disk.

A typical procedure for an icing run is as follows.

1. The target airspeed and total temperature were set.
2. The spray system pressures were set to give the desired MVD and LWC.
3. The spray system was turned on for the desired spray time.
4. The tunnel was brought down to fan idle for ice shape tracings and photographs.
5. The airfoil was then cleaned and the tunnel conditions set for the next data point.

#### Test Conditions:

Ice shape data will be shown for tests with an airspeed of 198 mph, an LWC of  $.6 \text{ g/m}^3$ , an MVD of  $20 \mu\text{m}$ , two temperatures ( $T_t = 17^\circ\text{F}$ , and  $30^\circ\text{F}$ ), two angles of attack ( $\alpha = 4^\circ$ , and  $8^\circ$ ), and three flap gap settings (1.52%, 1.75%, and 2.02% chord).

## RESULTS AND DISCUSSION

The 1994 McDonnell Douglas/NASA High-Lift Multi-Element test entry in the IRT was composed of 177 icing runs, as well as a number of clean airfoil angle-of-attack sweeps. Ice shape data and clean airfoil data discussed in this paper constituted a subset of the above mentioned database, and were obtained with the flap in the landing configuration (a flap deflection of  $30^\circ$ ). The results presented in this section will investigate the effect of the following parameters on the observed ice accretions: (1) angle-of-attack, and (2) size of flap gap.

#### Surface Pressure Distributions for the Clean Airfoil

128 static pressure orifices were installed in the model components and connected to the IRT ESP system, for the purpose of measuring clean airfoil pressure distributions. These orifices were distributed in a single chordwise row at model midspan on all three elements, and also in spanwise rows located on the upper surface of the slat (5 percent stowed chord) and flap (74 and 99 percent stowed chord). Observation of the spanwise pressure distributions provided an assessment of the level of two-dimensionality of the flow about the model.

Figure 3 presents a spanwise pressure distribution for the multi-element model obtained at a 4 degree angle-of-attack. The measured spanwise pressures indicate the two-dimensionality of the flow between 42 and 58 percent of the span, where the ice shape

tracings were obtained. Three-dimensional effects are most noticeable near the tunnel walls, where the measured spanwise pressures are non-uniform. This is particularly evident near the flap trailing edge.

Figure 4 is a comparison of chordwise pressure distribution for three angles-of-attack (4, 8, and 16 degrees). As the angle-of-attack is increased, the lift is increased on the main and slat elements, but the flap shows a reduction of lift with increasing angle of attack. These trends are consistent with measurements taken on a geometrically similar model in the LTPT.<sup>1,2</sup>

#### Ice Shape Results

Ice shape tracings were made at two spanwise stations on each element, which were 6 inches above and below the midspan. These two locations were chosen because the icing cloud is most uniform at the center of the test section. All of the ice shape tracings will be presented in terms of stowed, non-dimensionalized coordinates.

Spatial Uniformity: Figure 5 shows a comparison of ice shape tracings obtained at both spanwise locations from the same experimental run. These two ice shape tracings are typical of what might be considered the spatial uniformity for glaze ice shapes in this test. This close agreement suggests that it is valid to present the ice shape data in terms of one ice shape which is the average of both spanwise locations. Hereafter, ice shape data will be presented in the form of an "average" ice shape for each of the three elements (slat, main element, and flap).

Repeatability: Previous experimental tests on single-element airfoils, and multi-element airfoils have shown that the repeatability of ice shapes obtained in the IRT is quite good.<sup>5,7</sup> Repeat runs were also obtained for many of the present tests, to evaluate the repeatability of ice shapes. As in the 1993 test, the repeatability of the rime ice shapes was excellent, and the repeatability of glaze ice shapes was good.<sup>5</sup>

Figure 6 is a comparison of average glaze ice shapes from two different experimental runs, with identical icing conditions (i.e.- same air velocity, LWC,  $T_t$ , MVD, etc). A comparison of features and amount of ice illustrates the degree of ice shape repeatability between repeat runs of the same conditions.

Angle of Attack Effect: As one might expect, variations in the angle-of-attack had an effect on the slat, main element, and flap ice accretions. It was observed that a change in angle-of-attack yielded more dramatic changes in the ice shapes, than did a change

in the flap gap setting. To demonstrate the effect of angle-of-attack on ice accretion, it was decided to show ice tracing data obtained at one flap gap setting of 1.52% (Gap1). Results obtained with gap1 are typical of those for the other flap gap settings.

Figure 7 is an angle-of-attack comparison, obtained at a condition where  $V = 198$  mph,  $T_i = 17^\circ\text{F}$ ,  $\text{LWC} = .6$   $\text{g/m}^3$ ,  $\text{MVD} = 20$   $\mu\text{m}$ , spray time = 6 minutes, and flap gap setting = 1.52% (gap1). The ice accreted on all three elements for this condition was rime ice. As the angle-of-attack was increased from 4 degrees to 8 degrees, the entire slat ice shape shifted towards the slat lower surface, and main element ice peak appeared to move upstream on the main element. There was no significant difference between the flap ice shapes obtained at 4 or 8 degrees angle-of-attack.

Figure 8 is another angle-of-attack comparison obtained at a temperature of  $30^\circ\text{F}$ , with all other conditions the same as in Figure 7. For this warmer condition, glaze ice was accreted on all three elements. The slat ice shape shifted toward the slat lower surface, and the main element ice peak appeared to move upstream, with increasing angle-of-attack. These trends agree with those seen in Figure 7 for the colder temperature of  $17^\circ\text{F}$ .

Some features were noted in Figure 8, which had not been observed in the ice shapes obtained at the colder temperature of  $17^\circ\text{F}$  and shown in Figure 7. The flap ice peak appeared to shift slightly toward the flap lower surface, with increased angle-of-attack. Though not clearly evident in this figure, other data not shown indicated this trend. Also, runback rivulets were observed on the flap upper surface for both the 4 and 8 degree angle-of-attack runs.

Angle-of-attack effects on the ice shapes were more noticeable at the warmer conditions. At a temperature of  $30^\circ\text{F}$  and relatively high LWC's (e.g.  $.6$   $\text{g/m}^3$ ), the water may not freeze immediately upon impact, but flows somewhat before freezing. This process tended to make the ice peaks on the main element and flap more "horn-like". This will be discussed further in the Summary and Conclusions.

Evaluation of photographic data, revealed a distinct region of smooth ice on the main element for both temperature conditions of  $17^\circ\text{F}$ , and  $30^\circ\text{F}$ . The smooth ice zone was visible downstream of the main element leading edge, and parallel with it. This smooth zone on the main element was also noted during the 1993 IRT test of the multi-element model.<sup>5</sup>

It is believed that the stagnation line is contained within this "smooth ice zone". This smooth zone was observed at an approximate chordwise location ranging from  $x/c = .06$  to  $x/c = .13$  on the main element. This observation from the icing data appears to correlate with the main element stagnation point location from the clean airfoil pressure distributions. Figure 4 suggests an approximate location of  $x/c = .09$  for the main element stagnation line.

Photographs also revealed that the smooth ice zone became wider as the angle-of-attack was increased. This widening effect was evident at  $17^\circ\text{F}$  and  $30^\circ\text{F}$ , but its extent could only be quantified at the warmer temperature. This is because the ice in the smooth zone was clear at  $30^\circ\text{F}$ , and chordwise position marks inscribed on the model were more discernible. Photos of the  $30^\circ\text{F}$  runs indicated, at 4 degrees angle-of-attack, the smooth zone was relatively narrow and extended from  $x/c = .07$  to  $x/c = .11$ . When the angle-of-attack increased to 8 degrees, the smooth zone widened to approximately  $x/c = .06$  to  $x/c = .13$ . The apparent widening of this smooth region may have contributed to the forward movement of the main element ice peak at 8 degrees angle-of-attack.

A smooth ice zone was also observed on the flap, just downstream of the flap ice peak. This smooth ice zone was visible at both temperatures.

Generally speaking, slat ice shapes were most affected by changes in angle-of-attack. This is consistent with observations from the 1993 IRT test, which indicated the slat ice shapes were far more sensitive to angle-of-attack changes, than the main element or flap.<sup>5</sup>

Flap Gap Effect: One of the primary objectives of this test was to investigate the effect of various flap gap settings on the multi-element ice accretions. It was demonstrated from the 1993 test results, that the flap gap would not ice over.<sup>5</sup> However, it was desired to study the effect of small changes in the flap gap, relative to the ice accretions on the slat, main element, and flap. Therefore, multi-element icing data were obtained for several flap gap sizes: (1) gap1 = 1.52% chord, (2) gap2 = 1.75% chord, and (3) gap3 = 2.02% chord. Ice shape data obtained with a flap gap setting of gap3 were not available at all the conditions discussed in this paper, but will be shown where available.

Review of the ice shape data in Figures 9 thru 12 reveals slight changes in ice accretions as the gap setting is changed. If one considers the angle-of-attack

to be a first order effect on the multi-element ice accretions, then the gap effect could probably be considered to be of lesser order. In most cases, it was difficult to realistically discern significant changes in the ice shapes as the gap size was changed, especially at the colder temperature of 17 °F.

Figure 9 is a comparison of slat, main element, and flap ice shapes with two different gap sizes: gap1 = 1.52%, gap2 = 1.75%. These “averaged” tracings were obtained at a CFD condition where  $V = 198$  mph,  $T_i = 30^\circ\text{F}$ ,  $\text{LWC} = .6 \text{ g/m}^3$ ,  $\text{MVD} = 20 \text{ }\mu\text{m}$ , spray time = 6 minutes, and  $\alpha = 4^\circ$ . Comparing the gap2 ice shape with the gap1 ice shape, reveals a slight shift of the slat ice peak toward the upper surface of the slat, with increased gap size. Correspondingly, the slat upper surface icing limit moved further downstream.

Some very slight differences can be seen in the main element and flap ice peaks as the gap size is increased from gap1 to gap2. The main element ice peak appears to have shifted backwards very slightly. Also, the flap ice peak appears to have shifted slightly towards the flap upper surface. Other data not shown confirmed this trend.

Figure 10 is similar to Figure 9, with the exception that  $T_i = 17^\circ\text{F}$ . Ice tracings for 3 gap settings were available for this set of conditions: gap1 = 1.52%, gap2 = 1.75%, and gap3 = 2.02%. A comparison of gap2 and gap3 ice shapes, with respect to gap1, reveal no significant differences for the slat, main element, or flap ice shapes.

Figure 11 is a comparison of slat, main element, and flap ice shape tracings with two different gap sizes: gap1 = 1.52%, gap2 = 1.75%. These “averaged” tracings were obtained at a CFD condition where  $V = 198$  mph,  $T_i = 30^\circ\text{F}$ ,  $\text{LWC} = .6 \text{ g/m}^3$ ,  $\text{MVD} = 20 \text{ }\mu\text{m}$ , spray time = 6 minutes, and  $\alpha = 8^\circ$ . Increasing the gap size from gap1 to gap2, appears to shift the slat ice peak more towards the upper surface, thereby causing the upper surface icing limits to extend further downstream. It also appears that the slat ice shape experiences a greater shift toward the slat upper surface at  $\alpha = 8^\circ$  than at  $\alpha = 4^\circ$ . This can be seen by comparing the relative shift in the slat ice shapes shown in Figure 9 for  $\alpha = 4^\circ$ , and Figure 11 for  $\alpha = 8^\circ$ .

Figure 11 also indicated that the ice peak on the main element lower surface moved slightly downstream, while the ice peak on the flap leading edge appeared to move slightly towards the flap upper surface. The

trends on the slat and flap are consistent with those observed at 4 degree angle-of-attack in Figure 9.

Figure 12 is similar to Figure 11, with the exception that  $T_i = 17^\circ\text{F}$ . Ice shapes for 3 gap settings were available for this set of conditions: gap1 = 1.52%, gap2 = 1.75%, and gap3 = 2.02%. There was no noticeable change in the slat, main element, or flap ice shapes, with increasing flap gap.

Generally speaking, a change in gap size affected the multi-element ice accretions to a much smaller degree, than did changes in angle-of-attack. It was difficult to look for significant changes in the ice accretions due to flap gap changes, because the absolute magnitude of any observed differences in the ice shapes was small. This was especially true at the colder temperature, where the flap gap effect on the ice shapes was of the same magnitude as the ice shape repeatability shown in Figure 6.

Again, the ice shapes displayed more pointed ice peaks for the main element and flap at the 30°F temperature. Despite the more pointed icing peak on the flap at the warmer temperature, the gap was never blocked by ice, regardless of the gap setting.

## SUMMARY AND CONCLUSIONS

Selected results from the 1994 icing test of a multi-element airfoil have been presented. The effect of angle-of-attack and flap gap setting on multi-element ice accretions was investigated. Some key results from these investigations are listed below:

- The slat ice accretion was much more sensitive to angle-of-attack changes, than were the main element, or flap. The slat ice shape shifted toward the slat lower surface as the angle-of-attack was increased.
- Changing the flap gap setting had a smaller effect on the multi-element ice accretions than did changing the angle-of-attack.
- Only at the warmer temperature were gap effects noticeable, and at this temperature the slat ice shape exhibited the greatest degree of change due to flap gap setting. The slat ice shape appeared to shift slightly towards the slat upper surface when the gap setting was increased from gap1 to gap2.
- At the warmer temperature, the shift in the slat ice shape due to flap gap changes, appeared to

increase in magnitude as the angle-of-attack was increased.

Differences in ice shapes due to angle-of-attack effects or gap effects, were more observable at the warmer temperature of 30°F. For the conditions of these tests, the freezing fraction was about .7 at 17°F, and about .25 at 30°F. Therefore, at 30°F a greater fraction of the water did not freeze immediately upon striking the airfoil surface, but flowed along the surface some finite distance before freezing. The actual path of course would be dependent on the flowfield.

It is believed that the ice peaks observed on the main element and flap were more accentuated at the warmer temperature due to flowfield effects near the slat-main element gap and the main element-flap gap. These ice peaks were located near the leading edge, just forward of the smooth ice zone on the respective element. The phenomenon is believed to be the same in both instances:

*-The stagnation line on the main element or flap, is contained within the smooth ice zone on the respective element*

*-Water impinging slightly forward of the stagnation line is swept forward on the element surface toward the gap*

*-As the water approaches the gap, it is nearing the suction peak of the element where velocities are at a relative maximum*

*-Increased air velocity increases the convective heat transfer, thus augmenting the freezing process*

*-As one layer of water freezes, the next layer freezes on top of it, creating a "horn" and also acting like a "dam".*

A slight movement of the main element ice peak and the flap ice peak were observed, due to changes in the angle-of-attack or flap gap setting. At the warmer temperature of 30°F, this ice peak movement can be partially explained by the previously mentioned temperature effect. However, at the colder temperature of 17°F, the water tends to freeze on contact. Therefore, changes are more affected by particle trajectories. This suggests that slight changes in the ice accretion at colder temperatures, may be more representative of subtle flowfield changes (such as those induced by angle-of-attack, or flap gap changes).

Ice accretions were observed on the slat, main element, and flap, for the conditions tested. Similar results were observed in the 1993 IRT test of the multi-element model. It has been suggested that the ice accretions

observed on the flap lower surface may not be typical of natural icing conditions, because lower surface ice of this magnitude does not appear to have been reported on multi-element transport wings in natural icing conditions. There is very little, if any, data for natural in-flight ice accretions on multi-element airfoils at this time. It is not clear whether lower surface icing could occur under conditions which are currently outside the bounds of the existing database, or whether the lower surface ice accretions obtained in the wind tunnel are due to icing simulation/scaling issues. Therefore, additional work is required to investigate these effects.

#### REFERENCES

1. Valarezo, W.O., Dominik, C.J., McGhee, R.J., and Goodman, W.L., "High Reynolds Number Configuration Development of a High-Lift Airfoil," AGARD Conference Proceedings 415, pp. 10-1 to 10-8, October, 1992.
2. Valarezo, W.O., Dominik, C.J., McGhee, R.J., Goodman, W.L., and Paschal, K.B., "Multi-Element Airfoil Optimization for Maximum Lift at High Reynolds Numbers," AIAA Paper 91-3332, September, 1991.
3. Valarezo, W.O., Dominik, C.J., and McGhee, R.J., "Reynolds and Mach Number Effects on Multielement Airfoils," Fifth Symposium on Numerical and Physical Aspects of Aerodynamic Flows, Long Beach, January, 1992.
4. Valarezo, W.O., "High Lift Testing at High Reynolds Numbers," AIAA Paper 92-3986, July, 1992.
5. Shin, J., Wilcox, P., Chin, V., Sheldon, D., "Icing Tests on an Advanced Two-Dimensional High-Lift Multi-Element Airfoil," AIAA Paper 94-1869, June 1994.
6. Ruff, G.A., "Analysis and Verification of the Icing Scaling Equations: Analysis and Verification," AEDC-TR-85-30, Vol.1, March, 1986.
7. Shin, J. and Bond, T. H., "Repeatability of Ice Shapes in the NASA Lewis Icing Research Tunnel," Journal of Aircraft, Vol. 31, No. 5, pp.1057-1063, Sept-Oct, 1994.

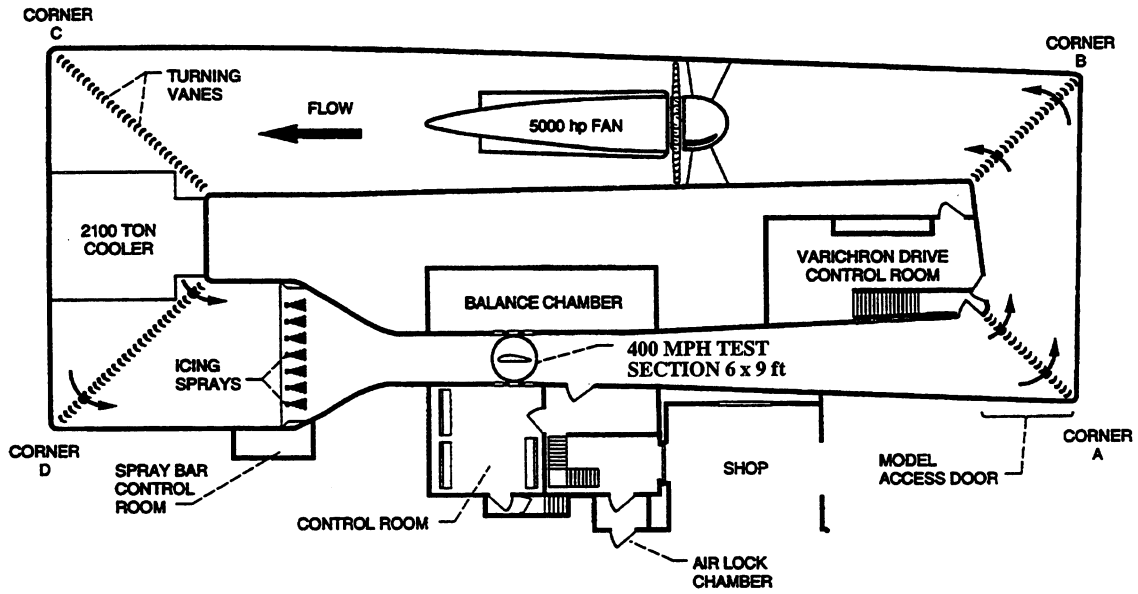


Figure 1 - Plan view of Icing Research Tunnel

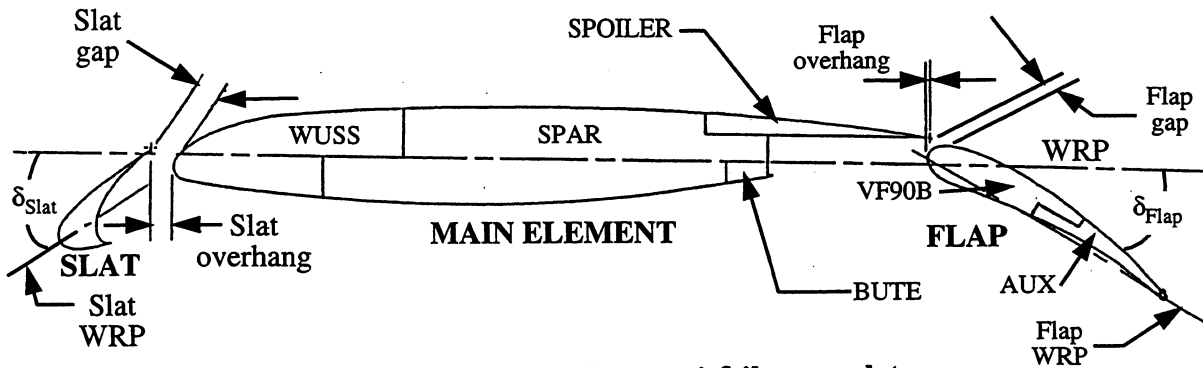


Figure 2 - Multi-element airfoil nomenclature

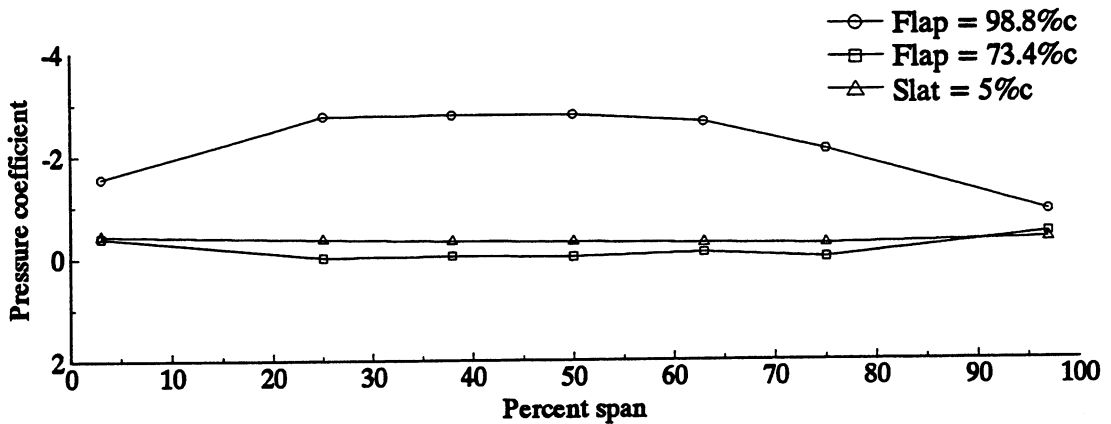


Figure 3 - Typical spanwise pressure distribution of the high-lift model

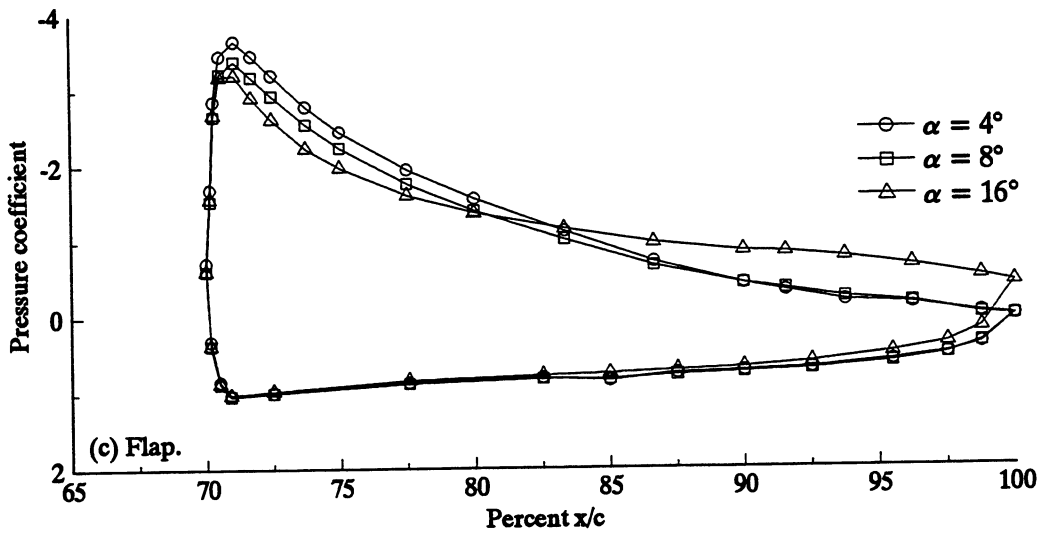
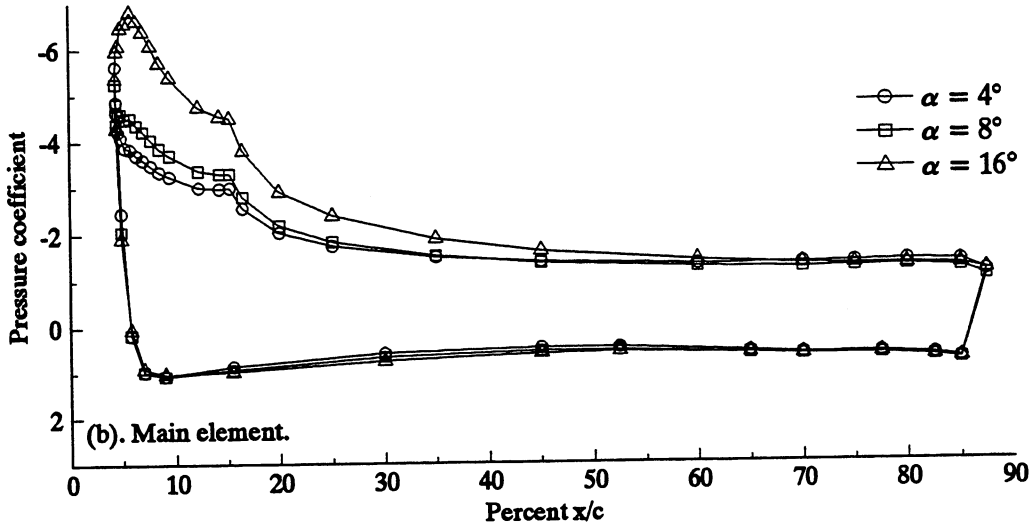
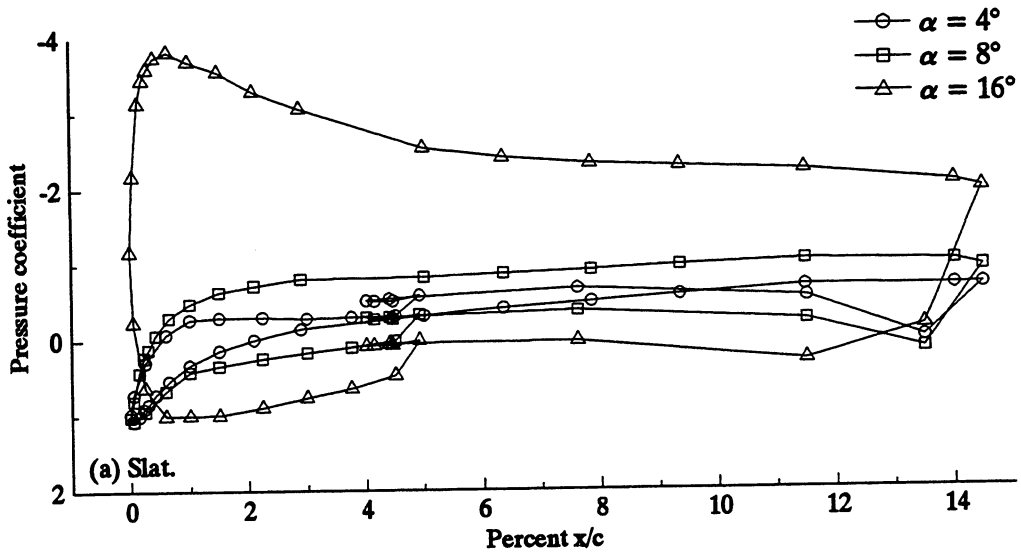
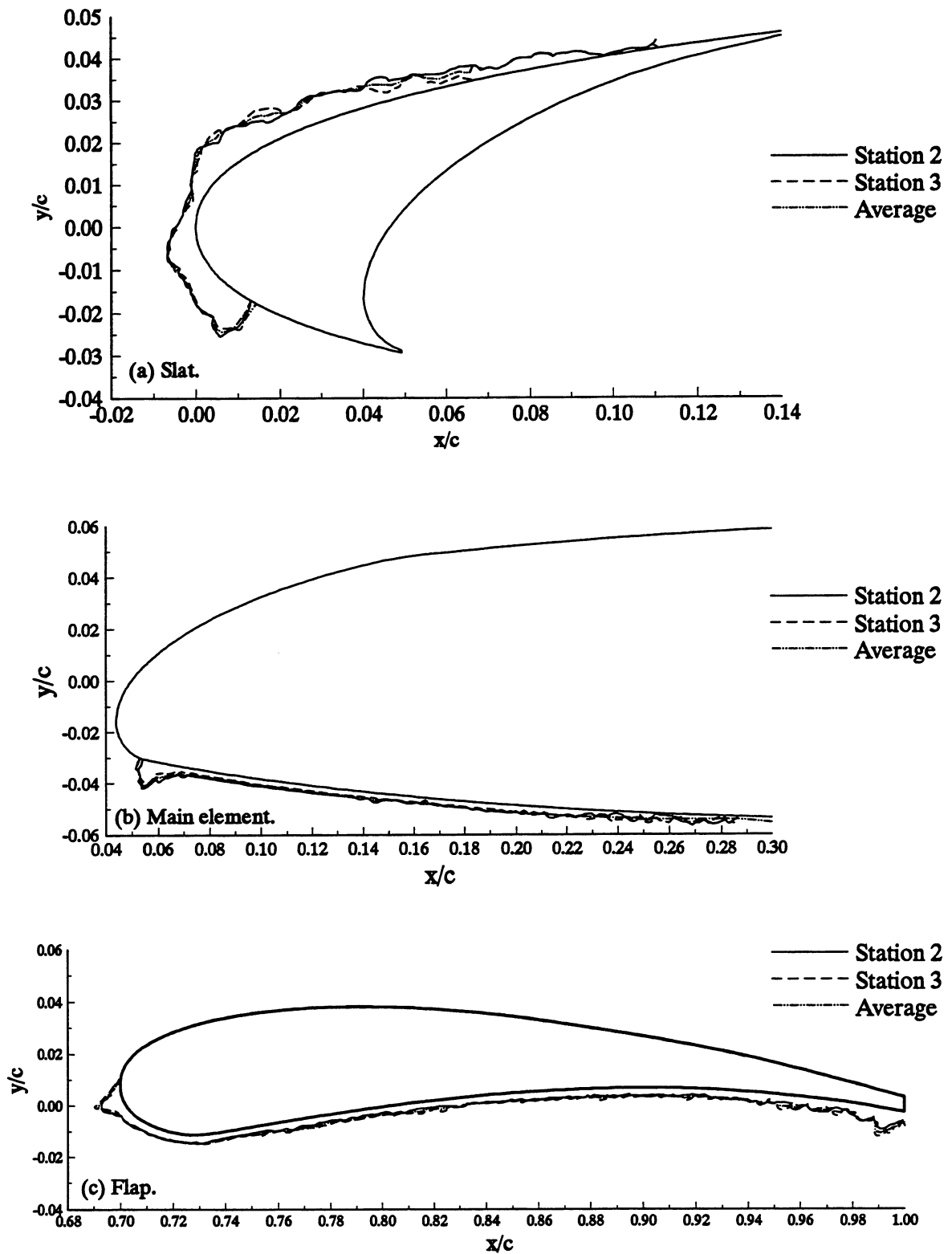
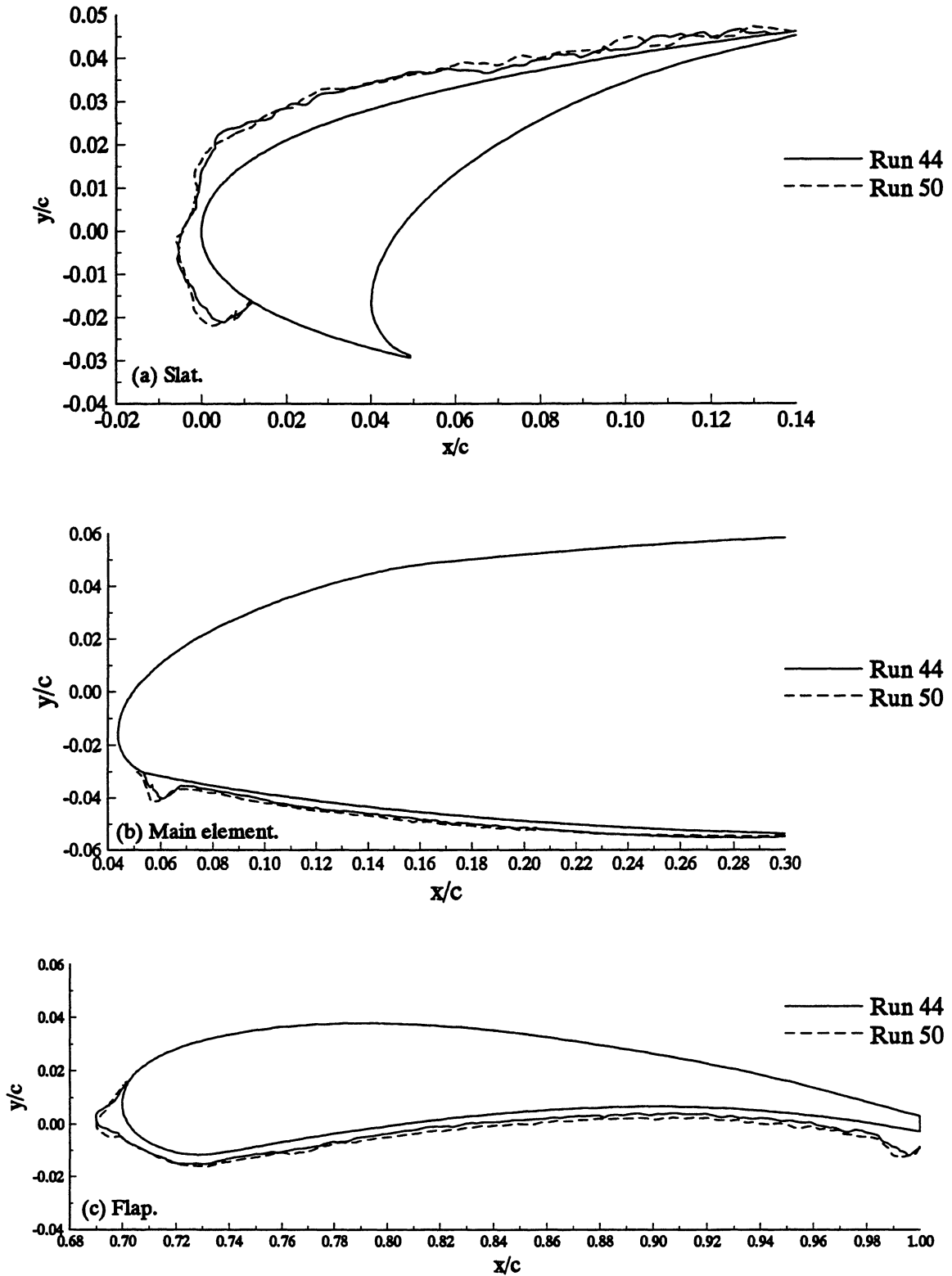


Figure 4 - Effect of angle-of-attack on high-lift model chordwise pressure distribution ( $V = 198$  mph,  $Re = 5.7 \times 10^6$ , gap 1)



**Figure 5 - Typical ice accretion spatial uniformity on high-lift model**  
 ( $V = 198$  mph,  $T_t = 30^\circ$ ,  $LWC = .6$  g/m<sup>3</sup>,  $MVD = 20$   $\mu$ m,  $\alpha = 4^\circ$ , gap 1,  $t = 6$  min)



**Figure 6 - Typical run-to-run ice accretion repeatability on high-lift model**  
 ( $V = 198$  mph,  $T_t = 30^\circ$ ,  $LWC = .6$  g/m<sup>3</sup>,  $MVD = 20$   $\mu$ m,  $\alpha = 4^\circ$ , gap 2,  $t = 6$  min)

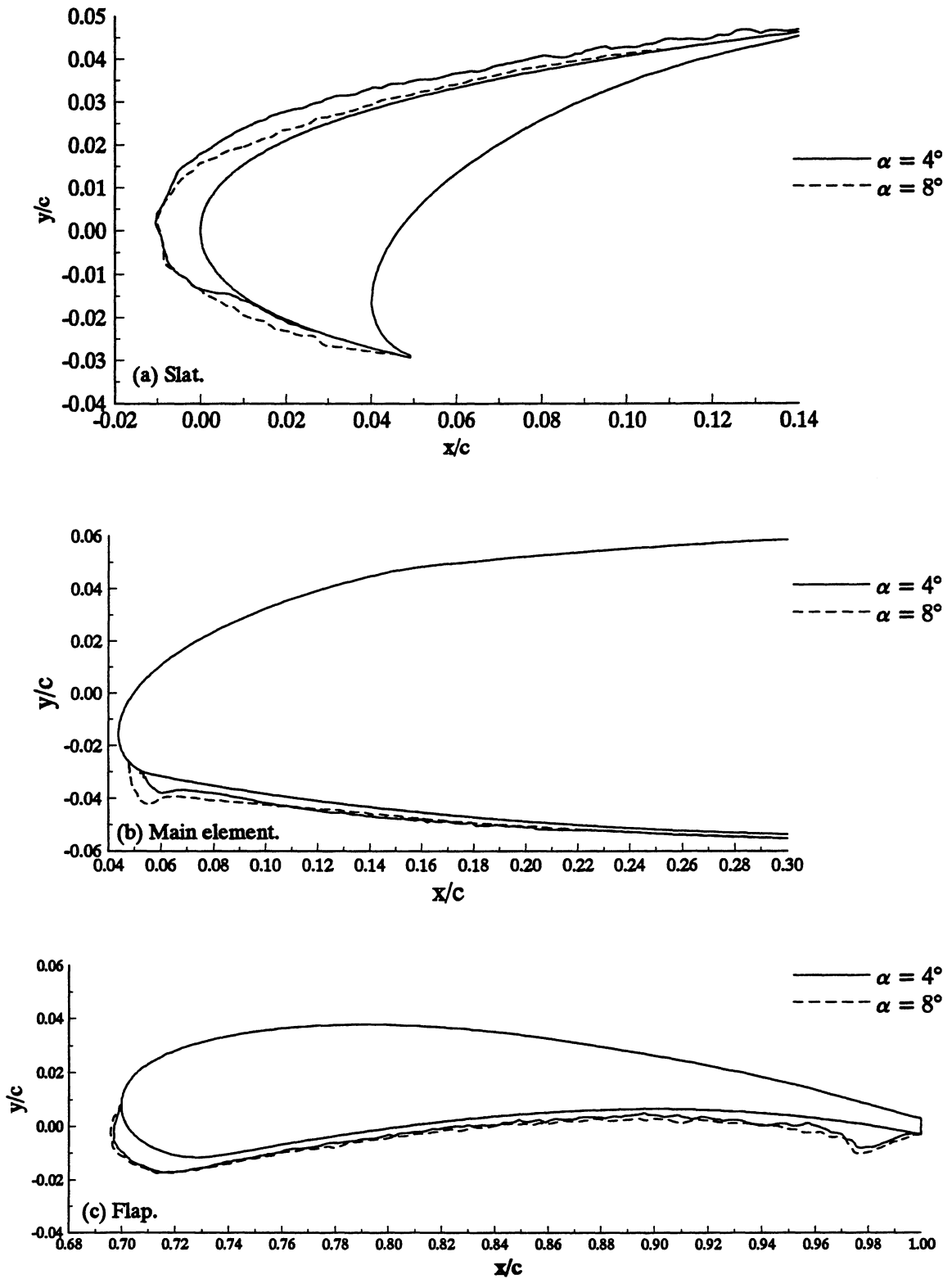


**Figure 7 - Effect of angle-of-attack on ice accretions**  
 ( $V = 198$  mph,  $T_t = 17^\circ$ ,  $LWC = .6$  g/m<sup>3</sup>,  $MVD = 20$   $\mu$ m, gap 1,  $t = 6$  min)

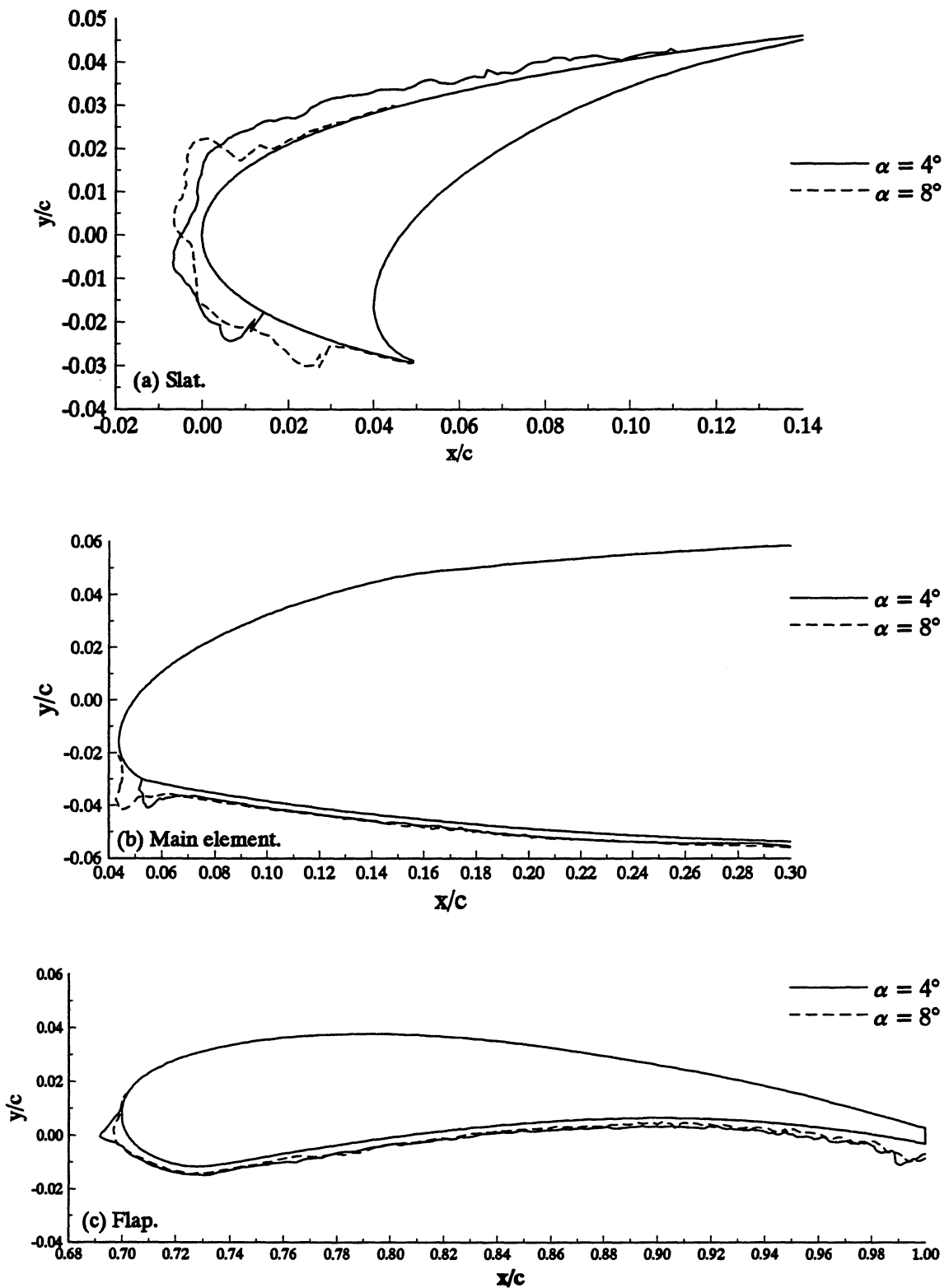


**Figure 8 - Effect of angle-of-attack on ice accretions**  
 ( $V = 198$  mph,  $T_t = 30^\circ$ ,  $LWC = .6$  g/m<sup>3</sup>,  $MVD = 20$   $\mu$ m, gap 1,  $t = 6$  min)

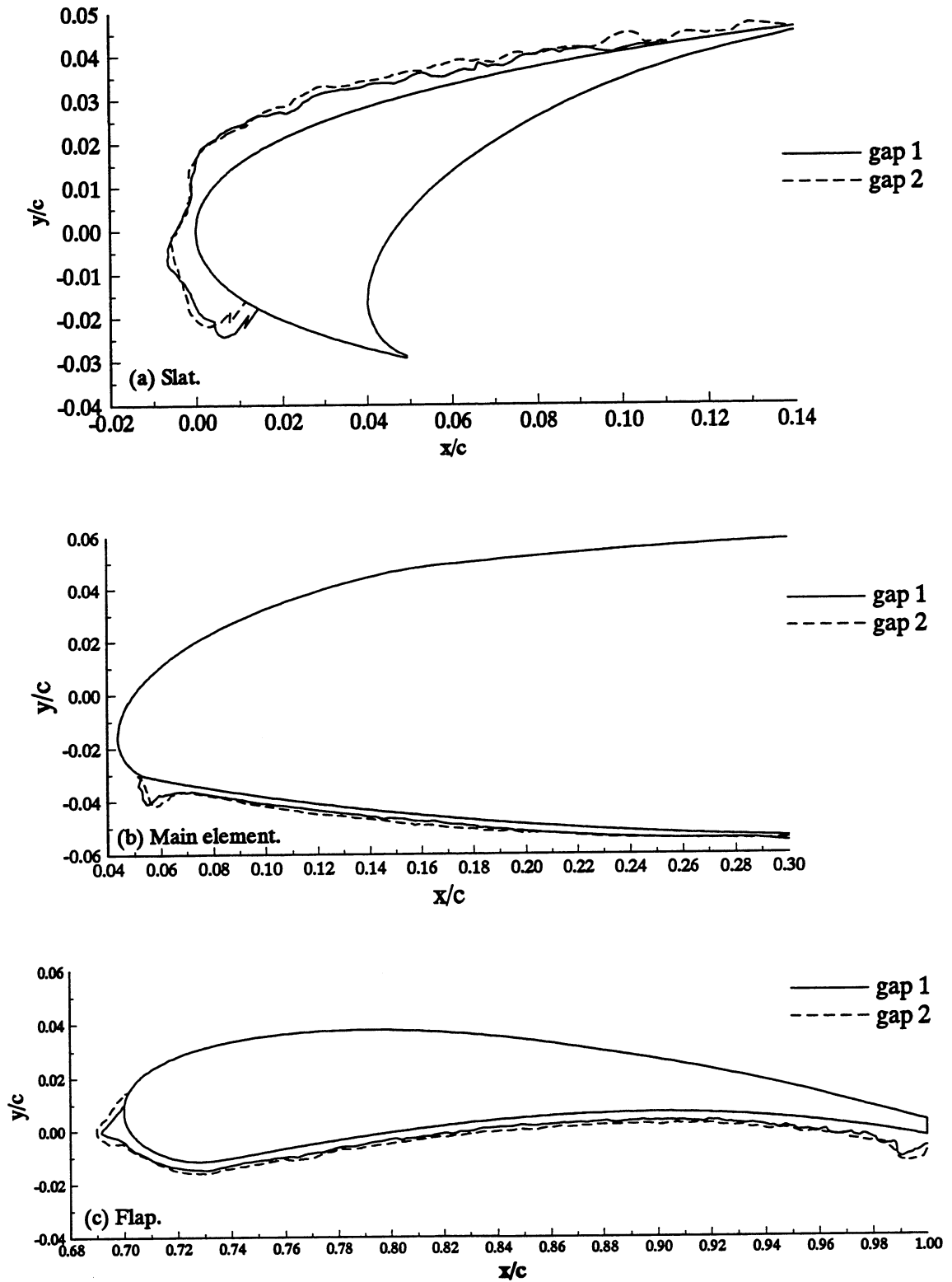


**Figure 9 - Effect of flap gap setting on ice accretions**  
 ( $V = 198$  mph,  $T_t = 30^\circ$ ,  $LWC = .6$  g/m<sup>3</sup>,  $MVD = 20$   $\mu$ m,  $\alpha = 4^\circ$ ,  $t = 6$  min)

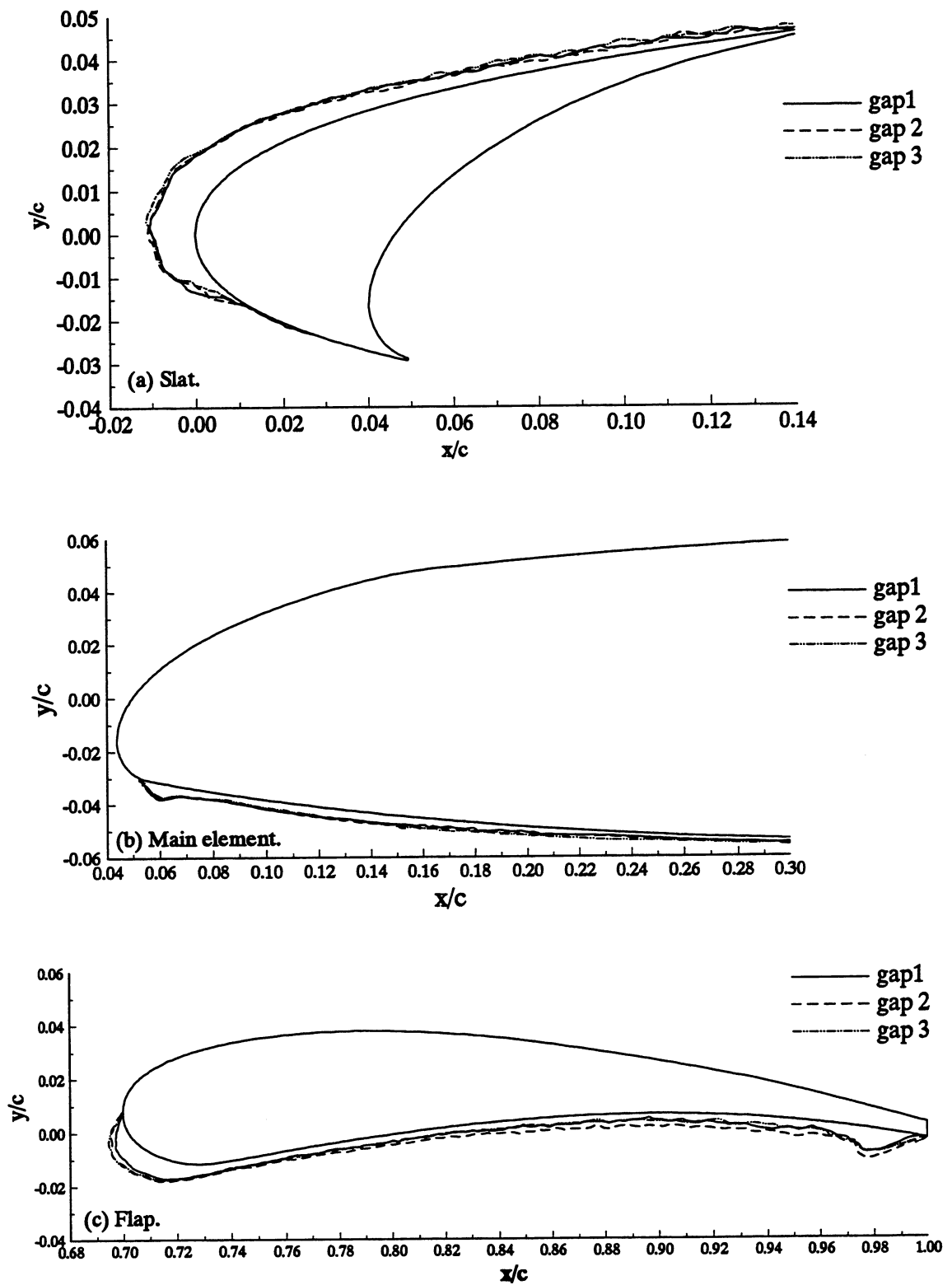


**Figure 10 - Effect of flap gap setting on ice accretions**  
 ( $V = 198$  mph,  $T_t = 17^\circ$ ,  $LWC = .6$  g/m<sup>3</sup>,  $MVD = 20$   $\mu$ m,  $\alpha = 4^\circ$ ,  $t = 6$  min)

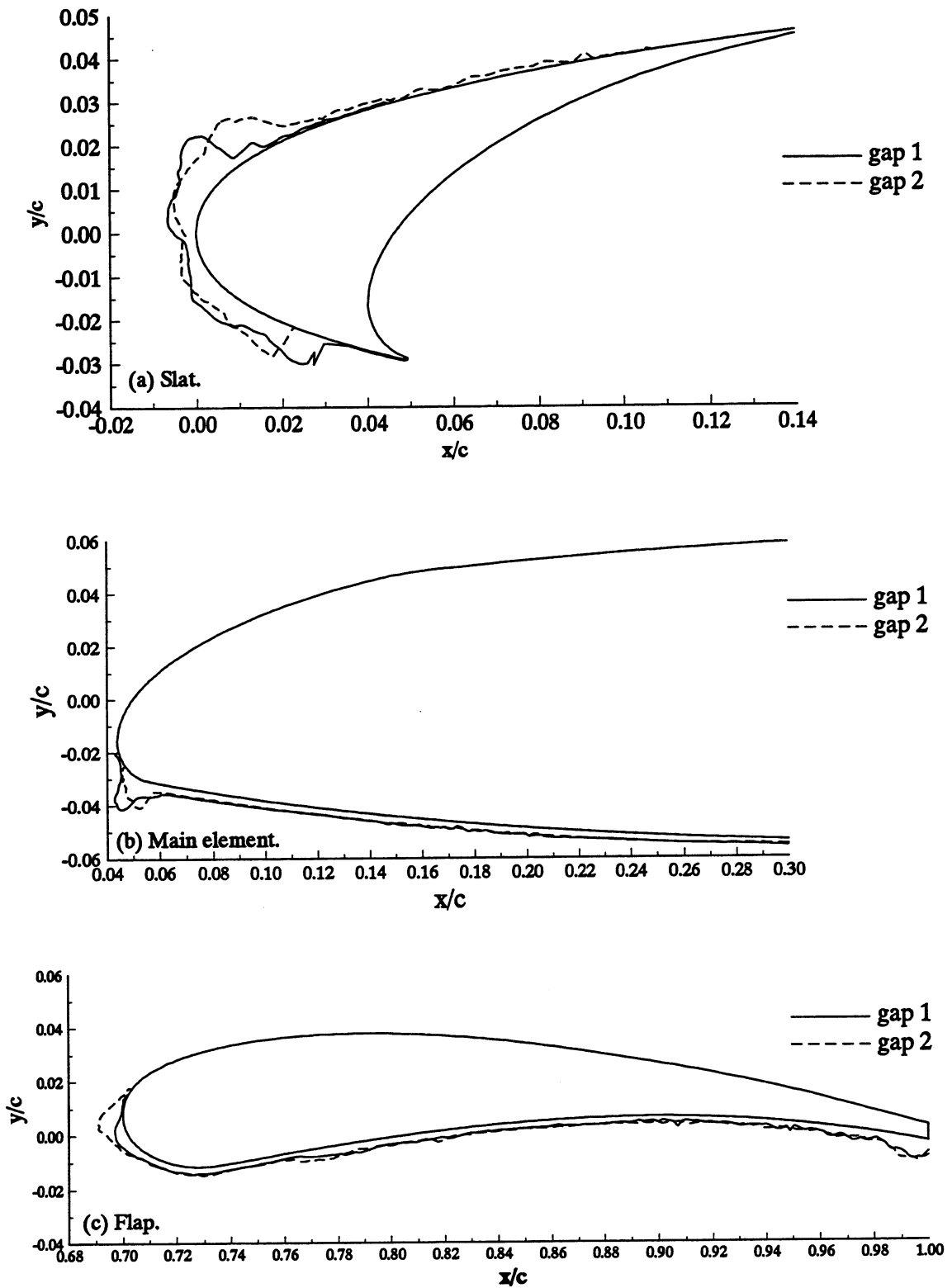


**Figure 11 - Effect of flap gap setting on ice accretions**  
 ( $V = 198$  mph,  $T_t = 30^\circ$ ,  $LWC = .6$  g/m<sup>3</sup>,  $MVD = 20$   $\mu$ m,  $\alpha = 8^\circ$ ,  $t = 6$  min)

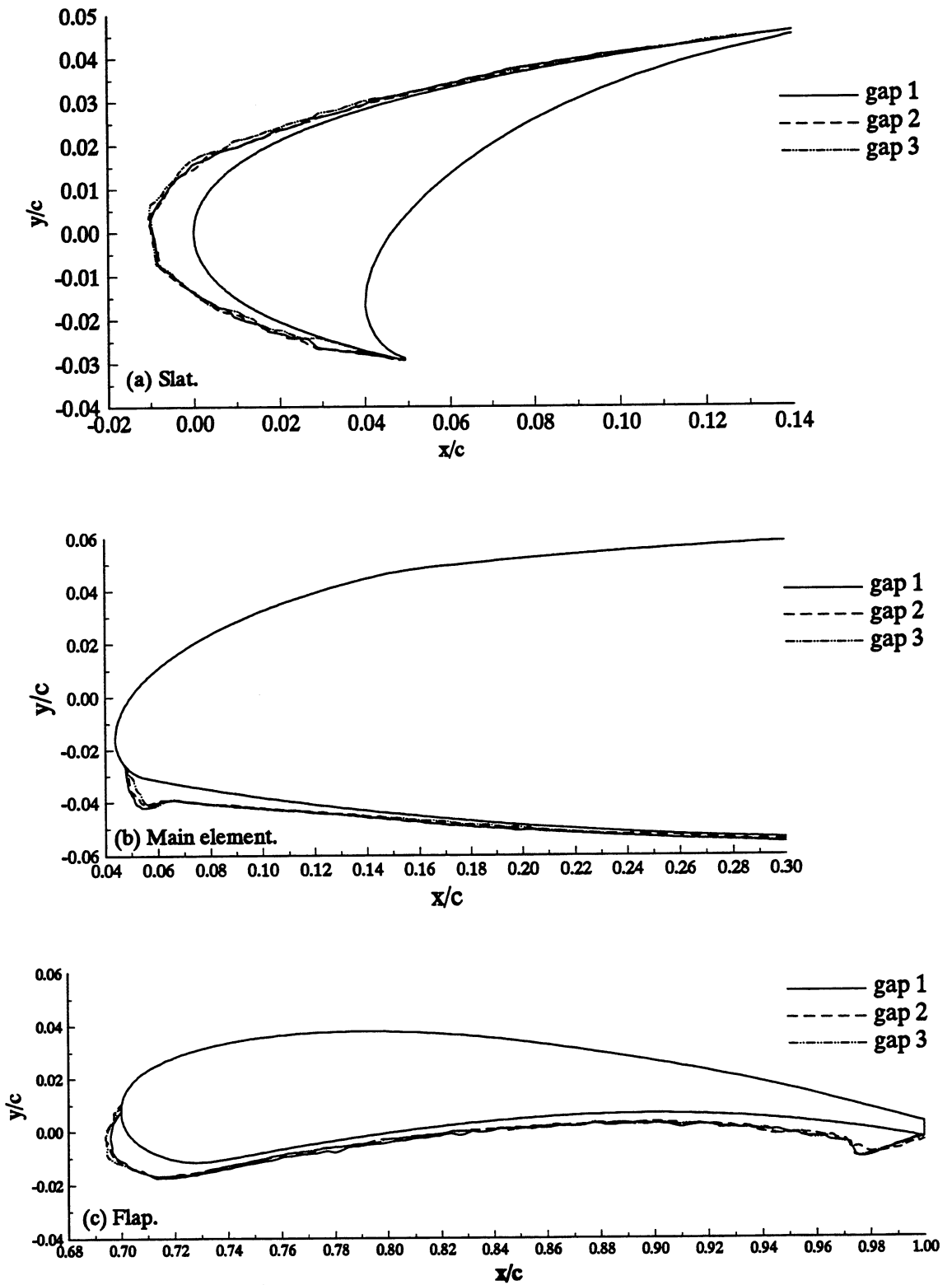


**Figure 12 - Effect of flap gap setting on ice accretions**  
 ( $V = 198$  mph,  $T_t = 17^\circ$ ,  $LWC = .6$  g/m<sup>3</sup>,  $MVD = 20$   $\mu$ m,  $\alpha = 8^\circ$ ,  $t = 6$  min)

# REPORT DOCUMENTATION PAGE

*Form Approved*  
OMB No. 0704-0188

Public reporting burden for this collection of information is estimated to average 1 hour per response, including the time for reviewing instructions, searching existing data sources, gathering and maintaining the data needed, and completing and reviewing the collection of information. Send comments regarding this burden estimate or any other aspect of this collection of information, including suggestions for reducing this burden, to Washington Headquarters Services, Directorate for Information Operations and Reports, 1215 Jefferson Davis Highway, Suite 1204, Arlington, VA 22202-4302, and to the Office of Management and Budget, Paperwork Reduction Project (0704-0188), Washington, DC 20503.

<b>1. AGENCY USE ONLY</b> ( <i>Leave blank</i> )		<b>2. REPORT DATE</b> May 1995	<b>3. REPORT TYPE AND DATES COVERED</b> Technical Memorandum	
<b>4. TITLE AND SUBTITLE</b>  Further Investigations of Icing Effects on an Advanced High-Lift Multi-Element Airfoil			<b>5. FUNDING NUMBERS</b>  WU-505-68-10	
<b>6. AUTHOR(S)</b>  Dean Miller, Jaiwon Shin, David Sheldon, Abdollah Khodadoust, Peter Wilcox, and Tammy Langhals				
<b>7. PERFORMING ORGANIZATION NAME(S) AND ADDRESS(ES)</b>  National Aeronautics and Space Administration Lewis Research Center Cleveland, Ohio 44135-3191			<b>8. PERFORMING ORGANIZATION REPORT NUMBER</b>  E-9683	
<b>9. SPONSORING/MONITORING AGENCY NAME(S) AND ADDRESS(ES)</b>  National Aeronautics and Space Administration Washington, D.C. 20546-0001			<b>10. SPONSORING/MONITORING AGENCY REPORT NUMBER</b>  NASA TM-106947 AIAA-95-1880	
<b>11. SUPPLEMENTARY NOTES</b>  Prepared for the Applied Aerodynamics Conference sponsored by the American Institute of Aeronautics and Astronautics, San Diego, California, June 19-22, 1995. Dean Miller, Jaiwon Shin, and David Sheldon, NASA Lewis Research Center; Abdollah Khodadoust and Peter Wilcox, McDonnell Douglas Aerospace, 1510 Hughes Way, Long Beach, California 90803; Tammy Langhals, NYMA, Inc., Engineering Services Division, 2001 Aerospace Parkway, Brook Park, Ohio 44142 (work funded by NASA Contract NAS3-27186). Responsible person, Dean Miller, organization code 2720, (216) 433-5349.				
<b>12a. DISTRIBUTION/AVAILABILITY STATEMENT</b>  Unclassified - Unlimited Subject Category 03  This publication is available from the NASA Center for Aerospace Information, (301) 621-0390.			<b>12b. DISTRIBUTION CODE</b>	
<b>13. ABSTRACT</b> ( <i>Maximum 200 words</i> )  In 1993 an experimental effort was initiated to investigate the effect of ice accretions on an advanced high-lift, multi-element airfoil. This airfoil is representative of an advanced transport wing, and has a state-of-the-art three element high lift system. This experimental effort is part of a cooperative program between McDonnell Douglas Aerospace and the NASA Lewis Research Center. The goal of this program is to improve the current understanding of ice accretion characteristics on multi-element airfoils. One key objective of this program is to establish an experimental database of multi-element ice accretions using the NASA-Lewis Icing Research Tunnel (IRT). The first multi-element icing test in this cooperative effort was conducted in 1993. A second "follow on" icing test was conducted in 1994, for the purpose of augmenting the multi-element ice accretion database obtained in 1993, and also for studying the effect of flap gap setting on ice accretions. This paper presents selected results from the 1994 multi-element icing test, and will emphasize the effect of angle-of-attack, and flap gap setting on multi-element ice accretions.				
<b>14. SUBJECT TERMS</b>  Icing; Aircraft hazards; Aeronautics; Multi-element airfoil			<b>15. NUMBER OF PAGES</b> 19	
			<b>16. PRICE CODE</b> A03	
<b>17. SECURITY CLASSIFICATION OF REPORT</b> Unclassified	<b>18. SECURITY CLASSIFICATION OF THIS PAGE</b> Unclassified	<b>19. SECURITY CLASSIFICATION OF ABSTRACT</b> Unclassified	<b>20. LIMITATION OF ABSTRACT</b>	